Journal of Thermal Analysis and Calorimetry, Vol. 65 (2001) 167–176

KINETIC AND THERMODYNAMIC PARAMETERS OF THE DECOMPOSITION OF CHROMIUM CHROMATE IN DIFFERENT GAS ATMOSPHERES

S. A. Halawy[1], *N. E. Fouad*[2], *M. A. Mohamed*[1*] *and M. I. Zaki*[3]

[1]Chemistry Department, Faculty of Science, South Valley University, Qena 83523, Egypt
[2]Chemistry Department, Umm al-Qura University, Mekkah Al-Mukaramah, P.O. Box 3711, Saudi Arabia
[3]Chemistry Department, Faculty of Science, Kuwait University, P.O. Box 5969, Safat, 13060 Kuwait

(Received February 5, 2001)

Abstract

Non-isothermal decomposition of chromium chromate hexahydrate, $Cr_2(CrO_4)_3 \cdot 6H_2O$, was studied on heating up to 600°C in different dynamic atmospheres of N_2, O_2 and H_2, using thermogravimetry (TG), derivative thermogravimetry (DTG) and differential scanning calorimetry (DSC). The results obtained at various heating rates (2–20°C min^{-1}) were used to derive kinetic (E_a and ln$A$) and thermodynamic (ΔH, C_p and ΔS) parameters.

It has been found that the activation energies of the dehydration and decomposition steps in N_2 are generally larger than in H_2 atmosphere, and the reverse is true for the enthalpy change of the decomposition. Thus, it has been concluded that the reductive decomposition (in H_2) is easier than the thermal decomposition (in N_2 or O_2) of the chromate. Irrespective of the gas atmosphere applied, the eventual decomposition product was a mixture of α-Cr_2O_3 and non-crystalline chromate species, γ-Cr_2O_{3+x}. Above 400°C in H_2 atmosphere, more deoxygenation of the non-crystalline chromate takes place at high rates of heating to give α-Cr_2O_3.

Keywords: chromium chromate, decomposition, DSC, kinetics, TG, thermodynamics

Introduction

Redox catalysis on calcined chromia based catalysts has been attributed [1–4] to formation of surface chromium chromate like species dwelling intimately coupled Cr^{III}–O and Cr^{VI}–O species (zone phase). The necessary localized adsorption of reactants on the surface has been considered [3, 4] to take place on coordinatively unsaturated Cr^{III} sites, and the electron availability to occur through electron-exchange interaction with nearby Cr^{VI}.

* Author to whom all correspondence should be addressed.

1418–2874/2001/ $ 5.00

Akadémiai Kiadó, Budapest
Kluwer Academic Publishers, Dordrecht

Therefore, a study performed in these laboratories of effects of the surroundings gas atmosphere (O_2, N_2 and H_2) on the thermal and chemical stability of a model chromium chromate hexahydrate compound, $Cr_2(CrO_4)_3 \cdot 6H_2O$, has recently been communicated [5]. A summary of the results obtained in the previous study [5], including the thermal and chemical characterization of the decomposition steps and identification of the products, is given in Table 1.

Table 1 Characteristics and assignments of thermal events encountered during the decomposition course of chromium chromate hexahydrate in N_2 atmosphere

Thermal step	T_{range}/°C	Mass loss/%	Assignment[a]
I	60–120	≈13	elimination of the six moles of water of hydration together with a minor deoxygenation leading to polymerization
II	120–370	≈12	
III	370–424	≈5.5	decomposition of bulk polychromates thus produced into non-stoichiometric γ-Cr_2O_{3+x}
IV	424–530	≈1.5	decomposition of γ-Cr_2O_{3+x} into a mixture of α-Cr_2O_3 and non-crystalline chromate species

[a]as suggested earlier [5]

The present study aims at calculating kinetic and thermodynamic parameters of the dehydration and decomposition steps of chromium chromate hexahydrate. In addition, it is also intended to study effects of the reducing atmosphere of H_2 on these parameters.

Experimental

Materials

The chromium chromate hexahydrate, $Cr_2(CrO_4)_3 \cdot 6H_2O$, was an AR-grade product of F. E. Decker (England) [5]. The purity of the reactant was 99.9% and, therefore, it was used as received.

Thermal analyses

Thermogravimetry (TG) and differential scanning calorimetry (DSC) were carried out, using respectively Shimadzu stand alone TGA-50H an DSC-50 analyzers (Japan) equipped with a data station model TA-50WSI. Highly sintered α-Al_2O_3 (Shimadzu Corp., Japan) was the thermally inert reference for DSC measurements. Calibration of the DSC analyzer was carried out, at different heating rates in N_2 and H_2 atmospheres, using the melting point and heat of fusion of pure indium (157°C and 28.24 J g^{-1} [6]) and zinc (419.7°C and 102 J g^{-1} [6]) products from Johnson Matthey (UK) and Aldrich (USA), respectively.

Comparable masses (ca 10–15 mg) of the test sample were used in all thermal analysis experiments to avoid effect of variation of the amount of sample on the peak shape and temperature [7]. Moreover, test samples were gently crushed, prior to analysis, to en-

sure particle size homogeneity and reproducibility of the results were also ensured. A constant flow rate (ca 40 ml min^{-1}) of different gases (N_2, O_2 and H_2) was applied. It should be stated here that the TG instrument was recalibrated at frequent intervals. Accuracy was always better than ±0.1 mg. Calibration of temperature for all instruments was always better than ±1°C in the different atmospheres applied. Using oxygen was not attempted in DSC experiments to avoid possible oxidation of the copper cell seats of the instrument. Platinum crucibles were used in all thermal analysis experiments. Therefore, no chemical interaction between the crucible material and the reactant salt was found to take place. The gases were 99.9% pure, and were supplied by the Egyptian Company of Industrial Gases (Helwan/Cairo). They were used as supplied.

Data processing

Kinetic parameters of the dehydration and decomposition steps of chromium chromate hexahydrate; namely, the activation energy (E_a/kJ mol^{-1}) and frequency factor (ln$A$/min) were calculated from derivative thermogravimetric curves (DTG) obtained at different heating rates (2–20°C min^{-1}), using Ozawa's equation [8]:

$$\ln\frac{\beta}{T_p^2} = -\frac{E_a}{RT_p} + \ln\frac{R}{\theta E_a}$$

where β is the heating rate (°C min^{-1}), T_p is the DTG peak temperature, R is the gas constant (8.314 J mol^{-1} K^{-1}), and θ is the reduced time=(1/A).

Thermodynamic parameters, i.e. enthalpy change (ΔH/J g^{-1}), heat capacity (C_p/J g^{-1} K^{-1}) and entropy change (ΔS/J g^{-1} K^{-1}) were calculated from DSC experiments carried out in N_2 and H_2 atmospheres at the different heating rates as follows. The enthalpy change was calculated directly from the amount of heat change involved in each step per unit mass of the test sample. ΔH thus determined was implemented to calculate the specific heat capacity (C_p) using the following equation [9]:

$$C_p = \frac{\Delta H}{\Delta T}$$

where $\Delta T = T_2 - T_1$, T_1 is the temperature at which the DSC peak begins to depart the base line, and T_2 is the temperature at which the peak lands [9]. Subsequently, the entropy change (ΔS) was calculated using the relationship:

$$\Delta S = 2.303 C_p \log\frac{T_2}{T_1}$$

Results and discussion

Thermal analysis of the decomposition course

Figure 1 displays TG and DSC curves obtained on heating at 5°C min^{-1} of $Cr_2(CrO_4)_3 \cdot 6H_2O$ in N_2 atmosphere. The TG curve monitors occurrence of four mass loss (ML)

steps (I–IV). The temperature range and amount of *ML* associated with each step are shown to be: I, 60–120°C; 13%; II, 120–375°C; 12%; III, 375–424°C; 5.5%; and IV, 424–530°C; 1.5%. The total *ML* in N_2 was determined to be 32% of the original mass of the test sample. The DSC curve shows step I to be endothermic with peak temperature (T_p) of 98°C, whereas the other three *ML* steps (II–IV) to be exothermic with T_p of 275, 385 and 435°C, respectively. The corresponding DTG curve (not shown) monitored consistently four *ML* peaks at 85, 281, 387 and 432°C.

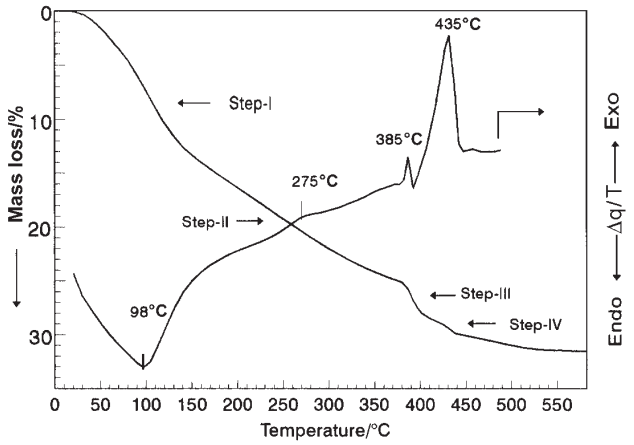

Fig. 1 TG and DSC curves of decomposition of $Cr_2(CrO_4)_3 \cdot 6H_2O$ obtained on heating at 5°C min^{-1} in a dynamic (40 mL min^{-1}) atmosphere of N_2

The decomposition in O_2 atmosphere [5] exhibited a TG curve monitoring similar steps to I and II at 70–370°C. Moreover, two steps similar to III and IV were shown, however, determining different *ML* values; namely, 2.5 and 3%, respectively.

Table 2 DSC peak temperature (T_p/°C) as a function of the heating rate (β/°C min^{-1}) in N_2 and H_2 atmosphere

β/°C min^{-1}	T_p in N_2				T_p in H_2	
	I (endo)	I (exo)	III (exo)	IV (exo)	I (endo)	II (exo)
2	87	268	374	422	76	256
5	98	275	385	435	83	272
7	106	280	393	442	–	–
10	115	290	399	447	98	288
15	122	295	404	451	103	302
20	126	298	412	457	107	306

DSC curves were obtained for $Cr_2(CrO_4)_3 \cdot 6H_2O$ at various heating rates (2–20°C min^{-1}) in N_2 atmosphere. The observed variation in T_p as a function of the

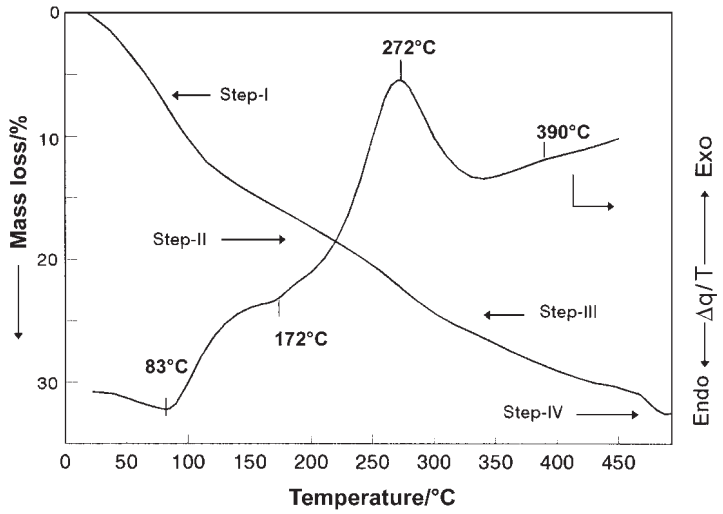

Fig. 2 TG and DSC curves of decomposition of $Cr_2(CrO_4)_3 \cdot 6H_2O$ obtained on heating at 5°C min^{-1} in a dynamic (40 mL min^{-1}) atmosphere of H_2

heating rate is shown for the events encountered in Table 2. Values of the corresponding enthalpy change (ΔH), and, hence those of C_p and ΔS, given in Table 3 were taken as the average of results of three experiments, for each heating rate both in N_2 and H_2 atmospheres. The kinetic parameters (E_a and $\ln A$), calculated from the variation of T_p of the DTG curves with the heating rate (in N_2 atmosphere), are also given in Table 3.

Figure 2 displays TG and DSC curves obtained on heating $Cr_2(CrO_4)_3 \cdot 6H_2O$ in H_2 atmosphere at 5°C min^{-1}. The TG curve is largely similar to that obtained in N_2 (or O_2), in showing four *ML* steps (I–IV). However, two differences can be observed.

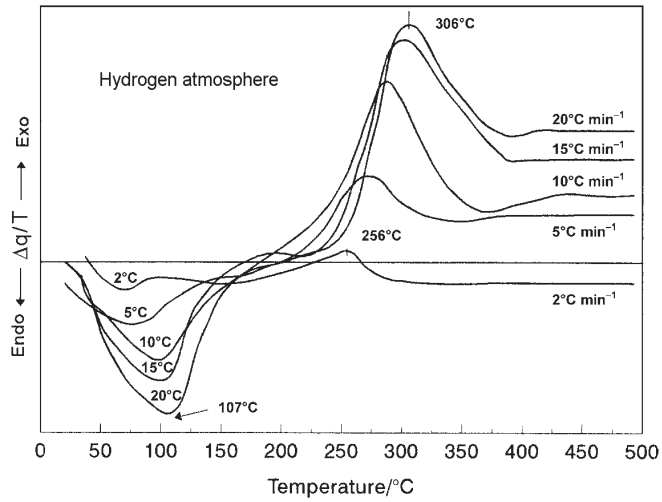

Fig. 3 DSC curves of decomposition of $Cr_2(CrO_4)_3 \cdot 6H_2O$ obtained on heating at the indicated heating rates in a dynamic atmosphere (40 mL min^{-1}) of H_2

Table 3 Kinetic and thermodynamic parameters for thermal events encountered during the decomposition course of chromium chromate hexahydrate in N_2 and H_2 atmosphteres

Parameter	Decomposition in N_2				Decomposition in H_2			
	Step I	Step II	Step III	Step IV	Step I	Step II	Step III	Step IV
E_a/kJ mol^{-1}	64.9±2	90.0±3	135.6±5	211.7±8	55.1±2	74.1±3	85.6±4	79.3±3
ln$A$/min^{-1}	19.7±0.6	31.6±1	20.5±0.6	34.8±1	17.1±0.6	21.1±0.7	15.1±0.5	10.9±0.4
Corr. coeff.	0.987	0.974	0.997	0.998	0.952	0.993	0.964	0.960
ΔH/J g^{-1}	193.2±7	–4.9±0.3	–5.0±0.3	–87.1±4	81.2±4	–119.9±6[a]		–4.44±0.6
C_p/J g^{-1} K^{-1}	1.40±0.15	0.11±0.01	0.16±0.02	1.5±0.1	0.64±0.06	0.80±0.08[a]		0.060±0.003
ΔS/J g^{-1} K^{-1}	0.69±0.03	–0.011±0.001	–0.010±0.001	–0.12±0.01	0.21±0.02	–0.22±0.02[a]		–0.0060±0.0002

[a] Cumulative results for overlapping step II and step III

Firstly, step III is overlapped with step II. Thus, it is enhanced to commence at a much lower temperature (250°C) than 375°C in N_2 or O_2. Secondly, step IV is slightly retarded in the presence of H_2 to commence above 470°C (instead of 424°C in N_2 or O_2). Also, the total *ML* was slightly different depending on the applied atmosphere, viz. 33% (H_2) >32% (N_2)>31.1% (O_2).

The corresponding DSC curve (Fig. 2) shows two main events, a broad endotherm maximized at 83°C, and a following strong and broad exotherm at 272°C. In addition, two weak responses appeared: an endothermic peak at 172°C, only observed at ≤5°C min^{-1}, and a very broad (weak) exothermic peak centered around 390°C.

Figure 3 displays DSC curves obtained for $Cr_2(CrO_4)_3 \cdot 6H_2O$ at different heating rates (2–20°C min^{-1}) in H_2 atmosphere. There appeared at >5°C min^{-1} a new weak, broad exotherm above 400°C. It gets sharper as the heating rate increases. The dependence of that peak on the heating rate is visualized in Fig. 4.

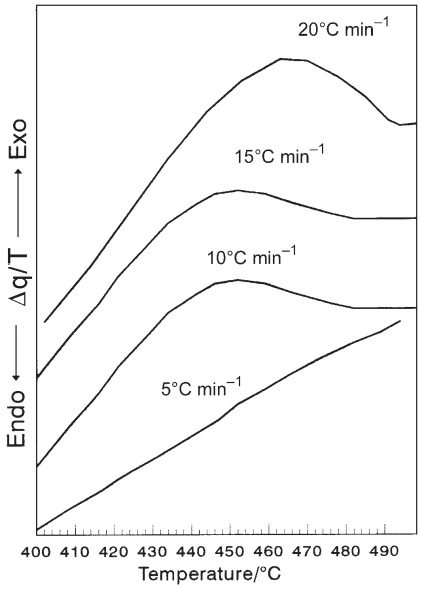

Fig. 4 DSC curves of decomposition of $Cr_2(CrO_4)_3 \cdot 6H_2O$ between 400–500°C obtained on heating at the indicated heating rates in a dynamic atmosphere (40 mL min^{-1}) of H_2

Variation of the DSC peak temperature (T_p) with the heating rate for all the thermal events observed is summarized in Table 2.

Kinetic and thermodynamic characteristics

Bearing in mind the assignments summarized in Table 1, the influence of the studied variables (gas atmosphere and heating rate) on the kinetic and thermodynamic parameters (Table 3) for each of the thermal events encountered is discussed below.

Step I, 60–120°C

The activation energy value (E_a=64.9 kJ mol^{-1}) suggests that the water molecules involved in the partial dehydration process undertaken in N_2 (O_2) atmosphere (Table 1) originate from loosely bound water of crystallization [11]. The positive sign of the corresponding entropy change (ΔS=0.69 J g^{-1} K^{-1}) is rather supportive. In H_2 atmosphere, however, the activation energy is reduced in magnitude (to 55.1 kJ mol^{-1}), and so is the corresponding enthalpy change (ΔH) (from 193.2→81.2 J g^{-1}).

The dehydration process in H_2 atmosphere started at appreciably lower temperature (≈15°C) than in N_2 or O_2 (≈13°C). It seems unlikely that this is due to a chemical involvement of H_2 molecules at such a low temperature regime (≤120°C), but may tentatively be ascribed to increased heat transfer and rapidity of diffusion of evolving H_2O molecules in the H_2 atmosphere [10].

Step II, 120–370°C

This process (*ML*≈12%) involves elimination of the remaining water molecules. The corresponding higher activation energy value (90 kJ mol^{-1}) than that of step I (ca 64.9 kJ mol^{-1}), may imply that the molecules released are relatively more strongly bound (possibly held in the inner coordination sphere of the chromium atoms) than those released in step I. The commulative *ML* of steps I and II (ca 25%) is larger than would be expected (≈19.3%) for the removal of six moles of water. Therefore, some deoxygenation has been suggested to take place during the occurrence of step II [5]. Oxygen release is expected to result in the formation of polychromates [12]:

$$(1+x)CrO_4^{2-} \rightarrow Cr_{1+x}O_{4+3x}^{2-} + xO$$

The net exothermic nature of the process (Fig. 1) is considered to be supportive to the occurrence of deoxygenation, provided that the exothermic deoxygenation process is stronger than the concurrent endothermic dehydration process. In H_2 atmosphere, step III is shown to be enhanced to eventually overlap with step II (Fig. 2). It has been suggested that the favourable conditions facilitated in the H_2 atmosphere for the deoxygenation process result in the immediate reduction of the anhydrous chromate (or polychromate) into Cr_2O_3 [5]. Therefore, the enthalpy change (ca 119.9 J g^{-1}) determined for step II (actually II+III) in H_2 is much larger than that (ca 4.9 J g^{-1}) determined in N_2 for step II only. Consistently, the activation energy that determined in N_2 (≈90 kJ mol^{-1}) is higher than that (≈74.1 kJ mol^{-1}) determined in H_2 atmosphere.

Step III, 370–424°C

The *ML* accompanying this step is dependent on the applied atmosphere (viz. 5.5% in N_2 and 2.5% in O_2). This has been attributed to the possibility that the product is largely non-stoichiometric and contains a varying amount of excess oxygen (Cr_2O_{3+x}) depending on the heating atmosphere [5]. In H_2 atmosphere, however, the process is shown (*vide supra*) to be enhanced remarkably, thus commencing at a much lower temperature (ca 250°C) than in N_2 or O_2 (ca 370°C). As it is mentioned above, the

larger ΔH and lower E_a values determined in H_2 than in N_2 atmosphere (Table 3) may account for the reductive decomposition of the polychromate throughout step III.

Step IV, 424–530°C

The activation energy determined for step IV in N_2 (≈211.7 kJ mol^{-1}) is much larger than in H_2 (≈79.3 kJ mol^{-1}). The process undertaken in N_2 has been described to involve the elimination of excess oxygen, leading to formation of nearly stoichiometric Cr_2O_3 [5]. The strong (and sharp) exothermic nature of step IV (Fig. 1) is similar to that marking the crystallization into α-Cr_2O_3 [13].

In H_2, however, the process undertaken occurs at a relatively higher temperature regime (ca 470–580°C) than in N_2 (ca 424–530°C). The maintenance of this step in H_2 may disclose that the reduction product still contains measurable proportions of non-stoichiometric γ-Cr_2O_{3+x}. It has been suggested that the product was not completely converted into crystalline α-Cr_2O_3 [5]. This is also concluded from the presence of the weak exothermic response in the DSC curve (Fig. 2) which was more detectable the higher the heating rate (≥10°C min^{-1}); (Fig. 4). This weak response could be attributed to deoxygenation of minority surface species of γ-Cr_2O_{3+x} to give crystalline α-Cr_2O_3 [2, 3]. Based on a recent study [14], this weak exotherm could be attributed to the reduction of some surface Cr^{3+} to Cr^{2+} species as a result of dissociative chemisorption of H_2 molecules and then spill over to induce reduction.

Conclusions

1. The appearance of two dehydration steps indicated that the six molecules of water in the chromium chromate crystal are not similarly bonded in the lattice.
2. Above 380°C, deoxygenation of the polychromate takes place to yield non-stoichiometric Cr_2O_3 (γ-Cr_2O_{3+x}). This is followed by elimination of excess oxygen to form a mixture of stoichiometric α-Cr_2O_3 and non-crystalline chromate species.
3. In H_2, deoxygenation process was enhanced to take place at much lower temperature. Above 450°C, the non-stoichiometric oxide deoxygenates further to form α-Cr_2O_3 and non-crystalline chromate species with possible reduction of surface Cr^{3+} to Cr^{2+} due to hydrogen spill over.

References

1 R. L. Burwell, Jr., G. L. Haller, K. C. Taylor and J. F. Read, Adv. Catal., 20 (1969) 1.
2 E. Ellison, J. O. V. Oubridge and K. S. W. Sing, Trans. Faraday Soc., 66 (1970) 1004.
3 A. Ellison and K. S. W. Sing, JCS Faraday Trans. I, 74 (1987) 2807.
4 M. I. Zaki, N. E. Fouad, J. Leyrer and H. Knözinger, Appl. Catal., 21 (1986) 359.
5 N. E. Fouad, S. A. Halawy, M. A. Mohamed and M. I. Zaki, Thermochim. Acta, 329 (1999) 23.
6 R. C. Weast (Ed.), Handbook of Chemistry and Physics, 62nd Ed., CRC Press, Florida, 1982, J. W. Dodd and K. H. Tonge, Thermal Methods, Analytical Chemistry by Open Learning, B. R. Currell (Ed.), Wiley, Chichester 1987.

7 M. A. Mohamed and S. A. Halawy, J. Thermal Anal., 41 (1994) 147.
8 T. Ozawa, J. Thermal Anal., 7 (1975) 601.
9 C. Heald and A. C. K. Smith, Applied Physical Chemistry, McMillan Press, London 1982, p. 473.
10 M. A. Mohamed, A. K. Galwey and S. A. Halawey, Thermochim. Acta, 323 (1998) 27.
11 A. V. Nikolaev, V. A. Lagvinenko and L. I. Myachina, Thermal Analysis, Vol. 2, R. F. Schwenker and P. D. Garn (Eds), Academic Press, New York 1969, p. 779.
12 T. V. Rode, Oxygen compounds of chromium catalysts, in: Thermal Analysis, J. P. Redfern (Ed.), Izd. Akad. Nauk, SSSR, Moscow 1962, McMillan, London 1965, p. 122.
13 J. D. Carruthers, K. S. W. Sing and J. Fenerty, Nature, 213 (1967) 66.
14 N. E. Fouad, J. Therm. Anal. Cal., 60 (2000) 541.